
[View Journal Online](#)
[View Article Online](#)

Reticular synthesis, topological studies and physicochemical properties of a 3D manganese(II) coordination network $[\text{Mn}_3(\text{BTC})_2(\text{DMSO})_4]_n$

Leonã da Silva Flores ¹, Roselia Ives Rosa ¹, Jefferson da Silva Martins ³,
 Roberto Rosas Pinho ³, Renata Diniz ² and Charlane Cimini Corrêa ^{1,*}

¹ Department of Chemistry, Federal University of Juiz de Fora, Juiz de Fora, 36036-900, Brazil
leonansf@hotmail.com (L.S.F.), roseliaives@hotmail.com (R.I.R.), charlane.cimini@ufjf.edu.br (C.C.C.)

² Department of Chemistry, Federal University of Minas Gerais, Belo Horizonte, 31270-901, Brazil
dinizr@gmail.com (R.D.)

³ Department of Physics, Federal University of Juiz de Fora, Juiz de Fora, 36036-900, Brazil
jeffersonsilvamartins@gmail.com (J.S.M.), rrpinho1959@gmail.com (R.R.P.)

* Corresponding author at: Department of Chemistry, Federal University of Juiz de Fora, Juiz de Fora, 36036-900, Brazil.
 Tel: +55.32.21023310 Fax: +55.32.21023314 e-mail: charlane.cimini@ufjf.edu.br (C.C. Corrêa).

RESEARCH ARTICLE



doi 10.5155/eurjchem.10.2.180-188.1882

Received: 16 April 2019
 Received in revised form: 20 May 2019
 Accepted: 28 May 2019
 Published online: 30 June 2019
 Printed: 30 June 2019

KEYWORDS

Manganese
 Trimesic acid
 Reticular synthesis
 Coordination polymer
 Coordination network
 Secondary building unit

ABSTRACT

In order to build a metal-organic framework with mixed ligands (acid-acid), a 3D coordination network based on manganese metal center was obtained $[\text{Mn}_3(\text{BTC})_2(\text{DMSO})_4]_n$; where BTC = Benzene-1,3,5-tricarboxylic acid and DMSO = Dimethylsulfoxide. The crystal structure was determined by single crystal X-ray diffraction, showing the assembly of a tridimensional 3,6-connected non-entangled polymeric network, with RTL topology. The secondary building unit (SBU) acts as a node of the 3-periodic expansion and involves carboxylate- and oxo-bridged metals. The DMSO employed in the synthesis is chemically involved in the coordination as a $\mu_2\text{-O}$ bridge between distinct manganese metal centers. The structural characterization of the material was supported by spectroscopic (infrared absorption and Raman scattering), thermal (TG, DTG, and DTA) and elemental analysis.

Cite this: *Eur. J. Chem.* 2019, 10(2), 180-188

Journal website: www.eurjchem.com

1. Introduction

Coordination networks (CNs) are a subclass of coordination polymers (CPs) able to form loops, cross-links or spiro-links that extend periodically in 1D, 2D or 3D. Metal-organic frameworks (MOFs) are a subclass of CNs that are capable of hosting guests in their vacancies, either through bonds or interactions [1,2]. This hierarchical taxonomy, in addition to topological studies of CPs, are strongly recommended by the International Union of Pure and Applied Chemistry (IUPAC); as it allows a complete description of the assembled system [3].

In this way, the design of MOFs may be an interdisciplinary challenge, involving principles of Reticular Chemistry (RC) and the techniques or experiments that will produce materials with specific topologies, pore size, and functionalities [4-6]. Generally, reticular synthesis of MOFs is based on *oxo*-metallic connectors or secondary building units (SBUs - polynuclear groups, geometrically defined), in which the components are

strongly bound and will drive the expansion [7,8]. Some basic knowledge of RC contemplates a series of principles, such as the *Geometric Design Principle*, which considers that most structures will be determined by the simplest geometric form. This principle can be demonstrated by the synthesis of edge-transitive nets (default nets) [9] or by isorecticular materials, with the same topology [10]. Moreover, the *Deconstruction Principle* allows the reduction of the structural complexity of an underlying net with a fundamental topology. If there is a wide variety of SBUs and polytopic ligands, these can be simplified as geometric forms (polygons, polyhedra, rods, etc.) determined by essential points for expansion of the net: the points of extension [11]. In addition, the *Minimal Transitivity Principle* is based upon the observation that underlying nets, generally, tend to present minimal transitivity [12]. The transitivity of a net gain in understanding the structure even in more complex networks. Minimal transitivity will be related to the simplest structural attribution.

Table 1. Crystal data and structure refinement for $[\text{Mn}_3(\text{BTC})_2(\text{DMSO})_4]_n$.

Parameters	$[\text{Mn}_3(\text{BTC})_2(\text{DMSO})_4]_n$
Empirical formula	$\text{C}_{26}\text{H}_{30}\text{S}_4\text{O}_{16}\text{Mn}_3$
Formula weight	891.56
Temperature (K)	293.11(10)
Crystal system	Monoclinic
Space group	$P2_1/c$
a, (Å)	10.2683(2)
b, (Å)	10.3933(2)
c, (Å)	16.6366(3)
β (°)	95.189(2)
Volume (Å ³)	1768.21(6)
Z	2
ρ_{calc} (g/cm ³)	1.675
μ (mm ⁻¹)	1.360
F(000)	906.0
Crystal size (mm ³)	0.25 × 0.07 × 0.04
Radiation	MoK α ($\lambda = 0.71073$)
The 2 θ range for data collection (°)	3.3 to 27.9
Index ranges	$-13 \leq h \leq 13, -13 \leq k \leq 13, -21 \leq l \leq 21$
Reflections measured	37629
Independent reflections	4178 [$R_{\text{int}} = 0.041$]
Restraints/parameters	0/227
Goodness-of-fit on F^2	1.04
Final R indexes [$I \geq 2\sigma(I)$]	$R_1 = 0.040, wR_2 = 0.0975$
Final R indexes [all data]	$R_1 = 0.0484, wR_2 = 0.1027$
Largest diff. peak/hole (e Å ⁻³)	1.92 / -0.78

Considering all the principles and approximations related to RC, it may be said that the strategies to build MOFs are not trivial and demand chemical knowledge.

In this sense, benzene-1,3,5-tricarboxylic acid or trimesic acid has been employed largely as a tritopic ligand to build MOFs, principally, due to its high coordination power [13,14]. Diversity of structures and functionalities has been reported in the literature [15,16]. Although a large number of structures based on trimesic acid have been reported, there is a challenge to build MOFs based on trimesic acid in addition to another ligand (mixed-ligand-MOFs) [17-19]. This illustrates the importance of proposing new strategies of synthesis and the comprehension of the assembly of these systems.

Therefore, the objective of this work is to present the reticular synthesis, characterization and structural description of a novel 3D Mn(II)-coordination network, built from trimesic acid and DMSO which exhibits interesting structural and topological attributes.

2. Experimental

All chemicals were reagent grade, obtained from commercial sources, and used without further purification. Benzene-1,3,5-tricarboxylic acid/trimesic acid (BTC), pentanedioic acid/glutaric acid (GLU), manganese acetate $\text{Mn}(\text{CH}_3\text{COO})_2 \cdot 4\text{H}_2\text{O}$, and the solvent dimethylsulfoxide (DMSO) were purchased from Sigma-Aldrich.

The synthesis was carried out by slow diffusion using a 1:1:1 stoichiometry, at room temperature. In a test tube, $\text{Mn}(\text{CH}_3\text{COO})_2 \cdot 4\text{H}_2\text{O}$ (0.3 mmol, 0.0519 g) was added to a mixture of 1.5 mL of deionized water and 0.5 mL of DMSO. A mixture of DMSO (3.0 mL) and deionized water (1.0 mL) was carefully added, forming a thin layer. Finally, a solution of BTC (0.3 mmol, 0.0396 g) and GLU (0.3 mmol, 0.0519 g) ligands in DMSO (4.0 mL), after having its pH modified by the addition of 1.5 mL of NaOH 1.0 M and was carefully added over the layers. The system was then maintained undisturbed at room temperature. After one week, single crystals were observed on the wall of the tube. The obtained solid was filtered off, washed with cold ethanol and air dried at room temperature. The initial purpose of this synthesis was to build a MOF with mixed ligands (BTC/GLU).

Catena-[bis(μ_5 -benzene-1, 3, 5-tricarboxylato)-bis(μ_2 -dimethylsulfoxide)-bis(dimethylsulfoxide)-tri-manganese]. Color: Colorless. Yield: 68 %. FT-IR (KBr, ν , cm⁻¹): 3010 ($\nu_{\text{CH}_{\text{ar}}}$), 2362

($\nu_{\text{CH-sp}^3\text{DMSO}}$), 2331 ($\nu_{\text{CH-sp}^3\text{DMSO}}$), 1623 ($\nu_{\text{COO}^-_{\text{as}}}$), 1587 (ν_{CC}), 1548 ($\nu_{\text{COO}^-_{\text{as}}}$), 1441 ($\nu_{\text{COO}^-_{\text{s}}}$), 1378 ($\nu_{\text{COO}^-_{\text{s}}}$), 1001 (ν_{SO}), 577 ($\delta_{\text{COH-DMSO}}$), 541 (ν_{MnO}), 386 (β - MnO_2). RAMAN (ν , cm⁻¹): 3007 ($\nu_{\text{CH}_{\text{ar}}}$), 1612 ($\nu_{\text{COO}^-_{\text{as}}}$), 1602 (ν_{CC}), 1550 ($\nu_{\text{COO}^-_{\text{as}}}$), 1454 ($\nu_{\text{COO}^-_{\text{s}}}$), 1377 ($\nu_{\text{COO}^-_{\text{s}}}$), 1007 (ν_{SO}), 386 (β - MnO_2). Anal. calcd. for $\text{Mn}_3\text{C}_{26}\text{H}_{30}\text{O}_{16}\text{S}_4$: C, 34.9; H, 3.3 %. Found: C, 32.1; H, 4.9%.

2.1. Instrumentation

Single crystal X-ray diffraction (SCXRD) measurement was carried out at room temperature, using a Supernova Agilent diffractometer, with Mo K α ($\lambda = 0.71073$ Å). The crystal structure was solved and refined by SHELXT 14/5 and SHELXL 18/1 programs [20-22] and the multiscan absorption correction was applied. Data collection, reduction, and cell refinement were executed by Crysallis RED, Oxford diffraction Ltd. Version 1.171.32.38 and are presented in Table 1. Hydrogen atoms were located in a difference Fourier map and were added in idealized positions and then refined according to the riding-model approach, with C-H = 0.95 Å and with $U_{\text{iso}}(\text{H}) = 1.2U_{\text{eq}}(\text{C})$ [23,24]. All non-hydrogen atoms were refined anisotropically. The representations of the crystal structure were drawn by Mercury 4.1.0 and ORTEP3 programs for Windows [25-28]. The topological analysis of the network was performed by ToposPro package [29,30]. The natural tiling was drawn using Systre and 3dt programs [31].

Powder X-ray diffraction experiment was carried out using a Bruker diffractometer (D8 Advance), with monochromatic Cu-K α radiation source, in the range from 5 to 55° (2 θ) and with the steps of 0.02° at 40 kV and 40 mA.

The infrared absorption (IR) spectra were collected using KBr disks in the range of 4000-400 cm⁻¹ on a Bruker Alpha FTIR spectrometer. The Raman (R) spectrum was obtained on a Bruker RFS 100 equipment with an Nd:YAG laser operating at 1064 nm.

Thermal analysis (TG/DTG/DTA) data were obtained through measurements on a Shimadzu DSC-60 thermal analyser, using a Shimadzu TGA-60 thermo-balance. Approximately 5.7 mg of the sample was placed in an alumina crucible and heated in N₂ atmosphere at 10 °C/min from 18 to 600 °C. Elemental analysis (CHN) was measured on a Perkin Elmer model 2400. Mass spectrometry matrix-assisted laser desorption / ionization (MALDI) experiments were performed

Table 2. Selected geometric parameters of the crystal structure of $[\text{Mn}_3(\text{BTC})_2(\text{DMSO})_4]_n$ *.

Bond distances (Å)			
Mn2-O2 ⁱⁱⁱ	2.1079 (19)	S1-O7	1.525 (2)
Mn2-O2 ^{vi}	2.1079 (19)	S1-C11	1.771 (5)
Mn2-O3	2.1203 (19)	S1-C10	1.791 (5)
Mn2-O3 ^v	2.1203 (19)	S2-O8	1.505 (3)
Mn2-O7 ⁱⁱⁱ	2.348 (2)	S2-C13	1.758 (5)
Mn2-O7 ^v	2.348 (2)	S2-C12	1.782 (5)
Mn1-O1	2.109 (2)	O3-C8	1.253 (3)
Mn1-O4 ^{iv}	2.142 (2)	O4-C8	1.248 (4)
Mn1-O8	2.168 (2)	O1-C1	1.258 (3)
Mn1-O7	2.218 (19)	O2-C1	1.249 (3)
Mn1-O5 ⁱⁱ	2.228 (2)	O6-C9	1.256 (4)
Mn1-O6 ⁱⁱ	2.306 (2)	O5-C9	1.266 (3)
Bond angles / °			
O2 ⁱⁱⁱ -Mn2-O2 ^{vi}	180.00 (10)	O1-Mn1-O4 ^{iv}	91.91 (9)
O2 ⁱⁱⁱ -Mn2-O3	90.38 (8)	O1-Mn1-O8	91.30 (10)
O2 ^{vi} -Mn2-O3	89.62 (8)	O4 ^{iv} -Mn1-O8	176.70 (10)
O2 ⁱⁱⁱ -Mn2-O3 ^v	89.62 (8)	O1-Mn1-O7	101.33 (8)
O2 ^{vi} -Mn2-O3 ^v	90.38 (8)	O4 ^{iv} -Mn1-O7	89.10 (9)
O3-Mn2-O3 ^v	180.0	O8-Mn1-O7	89.54 (9)
O2 ⁱⁱⁱ -Mn2-O7 ⁱⁱⁱ	90.93 (8)	O1-Mn1-O5 ⁱⁱ	158.12 (8)
O2 ^{vi} -Mn2-O7 ⁱⁱⁱ	89.07 (8)	O4 ^{iv} -Mn1-O5 ⁱⁱ	86.33 (8)
O3-Mn2-O7 ⁱⁱⁱ	84.19 (8)	O8-Mn1-O5 ⁱⁱ	90.96 (9)
O3 ^v -Mn2-O7 ⁱⁱⁱ	95.81 (8)	O7-Mn1-O5 ⁱⁱ	100.44 (7)
O2 ⁱⁱⁱ -Mn2-O7 ^v	89.07 (8)	O1-Mn1-O6 ⁱⁱ	99.95 (8)
O2 ^{vi} -Mn2-O7 ^v	90.93 (8)	O4 ^{iv} -Mn1-O6 ⁱⁱ	88.09 (9)
O3-Mn2-O7 ^v	95.81 (8)	O8-Mn1-O6 ⁱⁱ	92.08 (9)
O3 ^v -Mn2-O7 ^v	84.19 (7)	O7-Mn1-O6 ⁱⁱ	158.61 (7)
O7 ⁱⁱⁱ -Mn2-O7 ^v	180.00 (8)	O5 ⁱⁱ -Mn1-O6 ⁱⁱ	58.22 (7)

Symmetry code: (i) $x-1, y, z$; (ii) $x+1, y, z$; (iii) $-x-1, y-1/2, -z+3/2$; (iv) $-x+1, y+1/2, -z+3/2$; (v) $-x+1, -y+1, -z+2$, (vi) $x, -y+3/2, z+1/2$.

using a pulsed nitrogen ultraviolet laser ($\lambda = 337$ nm) of an AXIMA Performance MALDI-TOF MS (Shimadzu Biotech).

The time-of-flight mass spectrometer operated in a high vacuum chamber with a base pressure of about 1.0×10^{-7} mbar. The calibration utilized the alpha-cyano-4-hydroxycinnamic acid (CHCA) dissolved in water (50:50 v:v) milli-Q quality/acetonitrile with 0.1 % TFA (trifluoroacetic acid) at a concentration of about 5×10^{-2} mol/L. For MALDI-TOF MS measurements, samples were suspended in DMSO (20 μL) and the final suspension was added to 20 μL of the matrix solution. 0.5 μL of this mixture was deposited on the stainless steel multiprobe and allowed to dry before introduction into the mass spectrometer. The instrument was set in the high-resolution, positive reflector ion mode and scans were taken from 100 to 400 m/z .

3. Results and discussion

3.1. Crystal structure description

All crystallographic data for the compound are exhibited in Table 1 and all geometric parameters, such as bond distances and angles, are summarized in Table 2. Coordination polymer $[\text{Mn}_3(\text{BTC})_2(\text{DMSO})_4]_n$ crystallizes in the monoclinic crystal system, with the centrosymmetric space group $P2_1/c$, with BTC ligand totally deprotonated and coordinated to the Mn(II) and expanding the polymeric structure.

Figure 1a represents the coordination environment of a fragment of the crystal structure of compound $[\text{Mn}_3(\text{BTC})_2(\text{DMSO})_4]_n$. The asymmetric unit involves two distinct metal centers, Mn1 and Mn2, crystallographically independent and the analysis of geometric parameters suggests that both of them adopt a distorted octahedral geometry, in which Mn1 is highly distorted. The BTC ligand is hexadentate as a μ_5 -ligand, wherein the carboxylate group O5-C9-O6 coordinates to Mn1ⁱ in a chelating η^2 mode. The carboxylate group C1-O1-O2 bridges Mn1 and Mn2^{iv} in a μ_2 - η^1 : η^1 mode (with a *syn-syn* conformation) and the carboxylate group O3-C8-O4 is coordinated to Mn2 in the same way. Two DMSO ligands, crystallographically independent, (O7-DMSO and O8-DMSO) are coordinated to Mn1. Only O7-DMSO is bridges (μ_2 -O) the two metal centers Mn2 and Mn1ⁱⁱⁱ. Figure 1b represents the

polyhedrons Mn1O₆ and Mn2O₆, in which the distorted octahedral geometry is promoted by the coordination environment surrounding Mn1 and Mn2 metal centers: four oxygen atoms from the BTC ligand (Mn1-O1, Mn1-O4, Mn1-O5, Mn1-O6) and two oxygen atoms (Mn1-O7 and Mn1-O8) from the DMSO ligand, displaying an average Mn-O distance of 2.194(9) Å. The largest angular deformation involves the Mn1 metal center and is attributed to the chelating ring formation Mn1-O5ⁱⁱ-C9ⁱⁱ-O6ⁱⁱ. This exhibits the most acute angle, 58.22 (7) °, and the largest Mn-O bond distance as Mn2-O7ⁱⁱⁱ and Mn2-O7^v, 2.348 (2) Å. The secondary building unit (SBU) appears as an hourglass trinuclear unit that expands periodically and is represented in Figure 1c, wherein the manganese metal centers Mn1...Mn2 are separated by 3.632 Å. It is interesting to notice that other coordination compounds presenting this type of linear trinuclear unit exhibit a variable value of the Mn(II)...Mn(II) distance: ranging from 3.213, 3.207, 3.232 to 3.223 Å [32]; and from 3.370 and 3.715 Å [33] to 3.593 Å [34]. Another reported SBU assembly involves a different array where the non-linear unit forms a trinuclear prism with a comparable Mn(II)...Mn(II) distance of 3.572 Å [35]. The tridimensional expansion of the coordination network is shown in Figure 1d, in which the vacancies of the net are growing along the *a* axis, occupied by DMSO ligands (represented as spacefill). The dashed region emphasizes the SBU. It should be noted that the carboxylate involved in the *oxo*-bridge can also assemble an infinite linear *oxo*-bridging in SBUs of coordination compounds, with diverse dimensionalities. A 1D coordination compound with magnetic properties and thermal behavior based on pivalate ligand and the acetate counter-ion was assembled from infinite *oxo*-bridge-SBU expansion [36]. On the other hand, an important and already known 3D metal-organic framework, MIL-53, possesses a similar infinite SBU composed by infinite *oxo*-bridge involving terephthalate and water ligands expanding tridimensionally [37]. Comparison of the compound's SBU suggests that the one-directional expansion of the SBU is stopped by chelation with Mn1 metal center. The manganese-manganese bond distance observed in $[\text{Mn}_3(\text{BTC})_2(\text{DMSO})_4]_n$ is 3.602 Å.

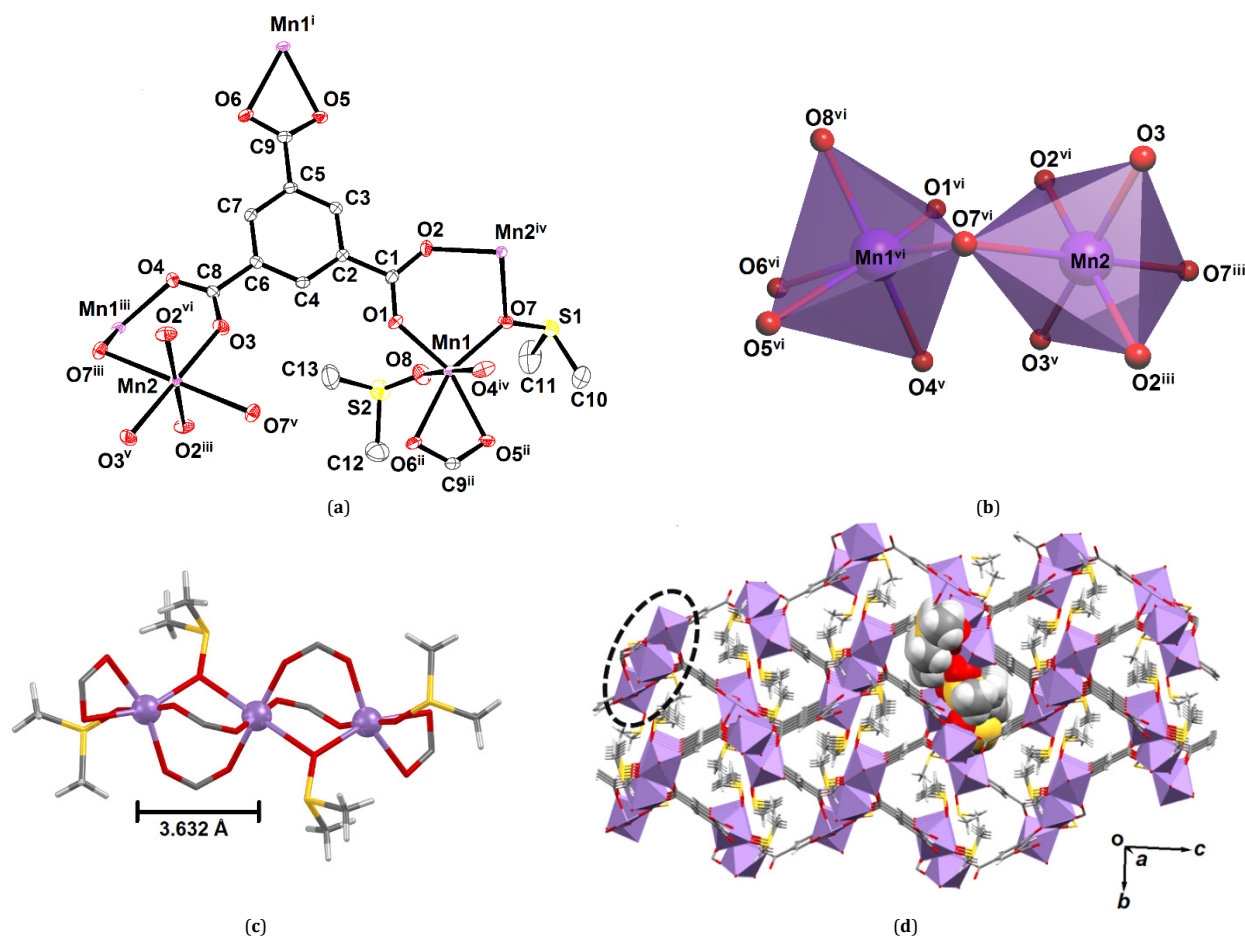


Figure 1. (a) Fragment of the crystal structure, emphasizing the asymmetric unit. The ellipsoids are represented with 30% of probability and hydrogen atoms were omitted for clarity. (b) Coordination polyhedral $Mn1O_6$ and $Mn2O_6$, representing the geometries of Mn1 and Mn2 metal centers (c) Hourglass trinuclear SBU, based on Mn(II) and (d) 3D expansion of the coordination network, representing DMSO ligands as spacefill and occupying the interior of vacancies. The SBU is highlighted by the dashed circle and Mn(II) metal centers are designed as polyhedral form. Symmetry code: (i) $x-1, y, z$; (ii) $x+1, y, z$; (iii) $-x-1, y-1/2, -z+3/2$; (iv) $-x+1, y+1/2, -z+3/2$; (v) $-x+1, -y+1, -z+2$, (vi) $x, -y+3/2, z+1/2$.

3.2. Topological analysis

The simplification used the cluster representation to consider the extension points on the SBU found. The connection of the extension points led to the octahedral and the triangular geometric solids (Figure 2a). 0-, 1- and 2-connected atoms do not contribute to the extension of the network and were omitted. Even if DMSO ligands participate in the coordination environment, they do not contribute to the topology of the net. Thus, the connection of the octahedral and triangular polyhedrons led to the simplified 3D network (Figure 2b); which is classified as a binodal 3,6-connected network, as shown in Figure 2c. The point symbol of this net is $(4.6^2)_2 (4^2 .6^{10}.8^3)$ and this topology type is reported in the topos&RCSR as rutile RTL framework, indicating that a default high symmetry net was obtained by the combination of octahedral and triangles [38]. We considered that the faces of the tiles display a set of channels that connect cavities. In the case of the manganese-coordination network, the face symbol for the tile is $[4.6^2]+[6^2.8^2]$, which means that 2 faces are 6-rings and that 1 face is a 4-ring, in the light blue tile (Figure 2d). The red tile is formed by 2 faces that are 6-rings and 2 faces that are 8-rings. This result is in accordance with the minimal transitivity principle [39], which states that the number of independent vertices and edges of the net must be as reduced as possible. The crystal structure determination was fundamental to describe these net characteristics.

3.3. Spectroscopic analysis

The approximate wavenumbers of the absorptions and their attributions are presented in Figures 3, 4 and Table 3 [40-42]. As observed, the presence of DMSO in the structure was suggested by the appearance of a pair of bands at 2361 and 1331 cm^{-1} , which are assigned, respectively, to the asymmetric and symmetric stretching mode of CH bond from the methyl group of DMSO. A band observed at 1001 cm^{-1} (IR) and 1007 cm^{-1} (R) was attributed to $\nu(SO)$ stretching of O-coordinated DMSO and the band located at 674 (IR) and 677 cm^{-1} (R) was attributed to $\nu(CS)$ symmetric stretching mode. IR and R spectra analysis of manganese-coordination network indicate the absence of the bands near 1721 cm^{-1} , characteristic of $\nu(COOH)$ stretching in the non-ionized carboxyl groups from BTC ligand, endorsing the non-protonated BTC^{3-} form in the structure. The asymmetric $\nu(COO^-)_{as}$ and symmetric $\nu(COO^-)_{s}$ stretchings were observed in the IR as a pair of bands at 1623 and 1548 cm^{-1} and 1441 and 1378 cm^{-1} , respectively. Therefore two $\Delta\nu = [\nu(COO^-)_{as} - \nu(COO^-)_{s}]$ [43] values referring to the coordination modes of carboxylate groups were determined. The value of the first, $\Delta\nu = 182 cm^{-1}$ is close to the value found for the ionic form of BTC ligand ($\Delta\nu = 183 cm^{-1}$) and suggests the bridging bidentate coordination mode. The other $\Delta\nu = 170 cm^{-1}$, may indicate the chelated bidentate coordination mode.

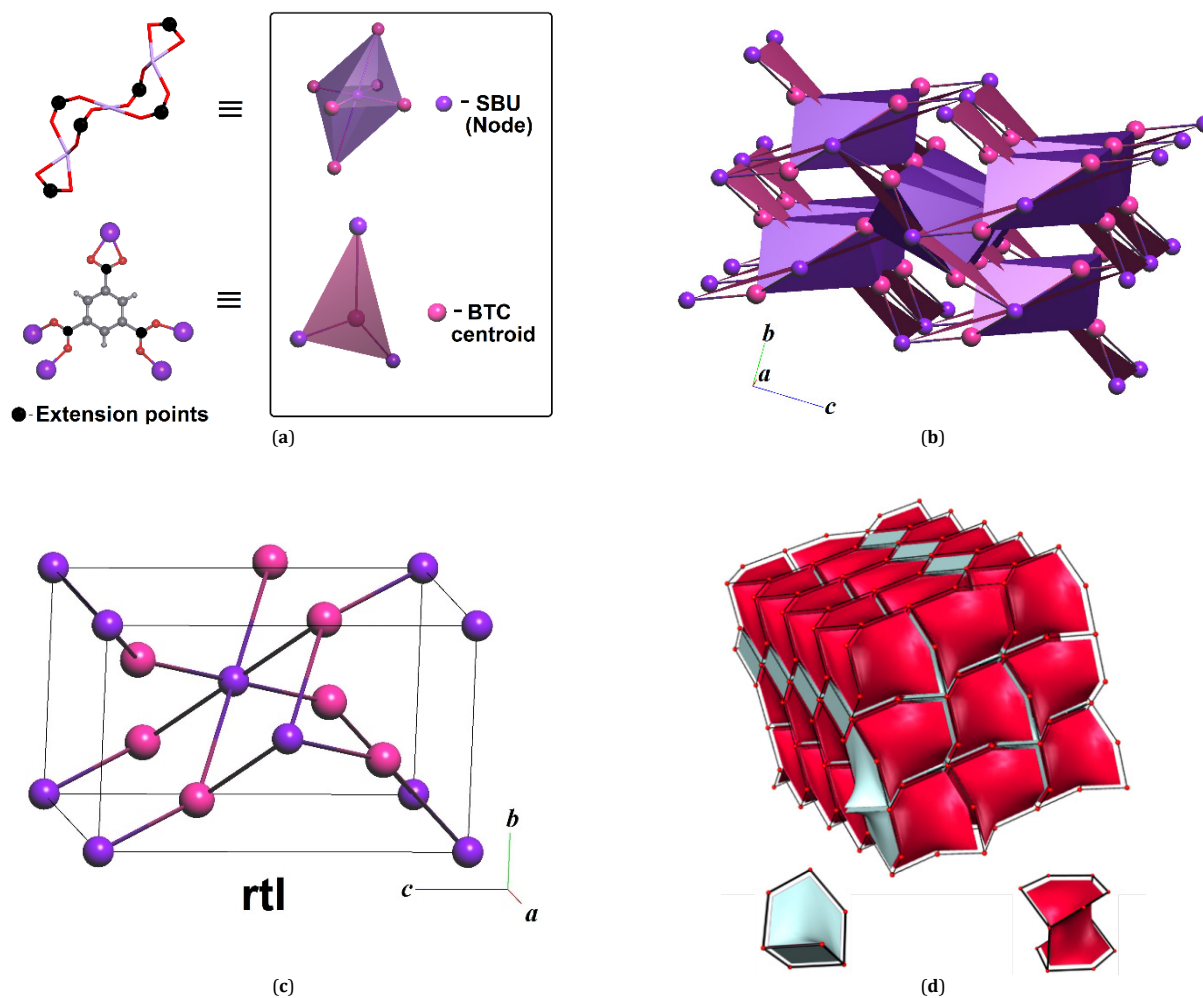


Figure 2. (a) The components of the 3D-coordination network, considering the $Mn_3(-CO_2)_6$ SBU as an octahedron and the tritopic BTC ligands as a triangle. (b) The combination of octahedral and triangles to assemble the RTL rutile-network. (c) Disposition of the nodes (SBU) and the ligands on the $P2_1/c$ unit cell. (d) Natural tiling for the crystal structure of $[Mn_3(BTC)_2(DMSO)_4]$, displaying the two kinds of tiles (light blue and red) and exhibiting the skeleton (vertices and edges).

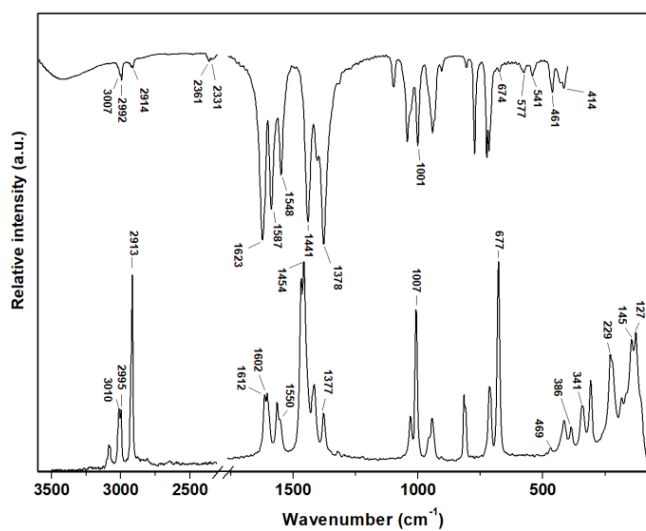
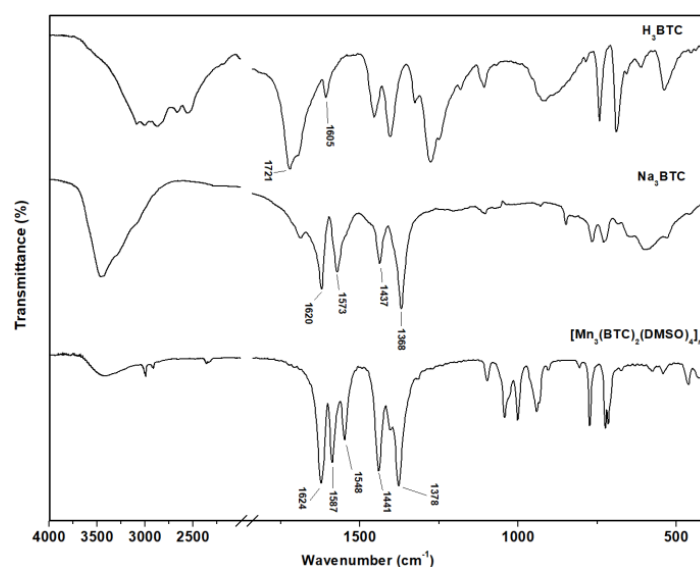


Figure 3. IR (upper) and R (bottom) spectra of the coordination compound. For R data collection, it was used 4 cm^{-1} of spectral resolution and 500 scans with a laser power of 10 mW.

Table 3. Selected vibrational wavenumbers (cm⁻¹) used as an attempt to assign the most important regions in the experimental spectra of compound *.

Vibrational Assignments	H ₃ BTC	Na ₃ BTC	[Mn ₃ (BTC) ₂ (DMSO) ₄] _n
v(CH) _{as} -DMSO			2361
v(CH) _s -DMSO			2331
v(SO)			1001 / 1007*
v(CS) _s			674 / 677*
v(MnO) _μ -DMSO			414 / 415*
δ(CO) _μ -DMSO			577
v(COO) _{as}		1620	1623 / 1612*, 1548 / 1550*
v(COO) _s		1437	1441 / 1454*, 1378 / 1377*
v(COOH)	1721		
Δv		183	182, 170
v(CC) _{ar}	1605	1573	1587 / 1602*
v(MnO)			541
β(Mn-O-Mn)			386*, 341*

* Raman bands are emphasized as *, as = asymmetric, s = symmetric, ar = aromatic, v = stretching, β = bending, δ = rocking.

**Figure 4.** IR spectra of the protonated form of BTC ligand, a sodium salt of BTC ligand and [Mn₃(BTC)₂(DMSO)₄]_n.

The O-coordination related to the v(MnO) stretching mode was assigned to the two bands observed at 309 and 341 cm⁻¹ in the Raman spectrum.

3.4. PXRD and thermal (TG/DTA) analysis

The comparative analysis between PXRD patterns from the sample and the simulated pattern (obtained from SCXRD data), showed the similarities and a good correspondence of the crystalline phases (Figure 5). It is important to emphasize the crystalline phase purity of the sample.

The thermal curves TG, DTG and DTA of [Mn₃(BTC)₂(DMSO)₄]_n are displayed in Figure 6. The DTG curve was used as an auxiliary for analysis of the TG data, which suggests that the compound is stable up to 250 °C. The two first and well-defined weight losses, were observed from 250 to 375.4 °C (obs. 17.1 %, calc. 17.5 %) and from 375.4 to 460.8 °C (obs. 17.7 %, calc. 17.5 %) and are attributed to the loss of 2 mol of DMSO. They are endothermic events, observed in the DTA curve. The distinct temperatures to remove the 2 mol of DMSO may suggest that the μ₂-O bridging ligand is binding to the metal center more weakly. In the temperature range from 460.8 to 569.2 °C, two intense exothermic events were observed and attributed to thermodecomposition of BTC ligand, involving CO₂ (3 mol), C₆H₃ (1 mol) and 1 mol of C₉H₃ (obs. 35.2 %, calc. 34.3 %). The final residue was consistent with 3 mol of manganese dioxide per mol of [Mn₃(BTC)₂(DMSO)₄]_n (obs. 30.4 %, calc. 29.3 %).

3.5. Time of flight mass spectrometry (TOF-LDI)

The preliminary analysis by time of flight mass spectrometry (TOF-MS) was carried out involving the laser desorption/ionization (LDI). This analysis is based on the mechanism of laser irradiation over a sample incorporated into a matrix capable of absorbing energy in the ultraviolet region. This technique is largely employed in the analysis of large molecules [44] however, analysis of small molecules has been limited by the interference of the matrix signal [45,46]. Thus, new platforms which do not depend on the matrix have been developed, aiming to eliminate the interferences that may be produced. These novel platforms should be capable of producing a minimal background signal, generally at less than 500 Da, allowing the application in the MALDI (Mass spectrometry matrix-assisted laser desorption/ionization) to identify small molecules [47].

The mass spectrum obtained (Figure 7) suggests that [Mn₃(BTC)₂(DMSO)₄]_n is fragmented in different ions with mass/charge (*m/z*) ratio, the most abundant being 285. The LDI-TOF experiment used a pulsed laser of N₂ (λ = 337 nm), showing that the compound absorbs the laser energy in at wavelength and produces desorption/ionization without the necessity of a matrix. Consequently, this result may suggest some potential to the application of this material as a matrix in the MALDI technique in the analysis of small molecules, for example, small molecular weight pollutants [48].

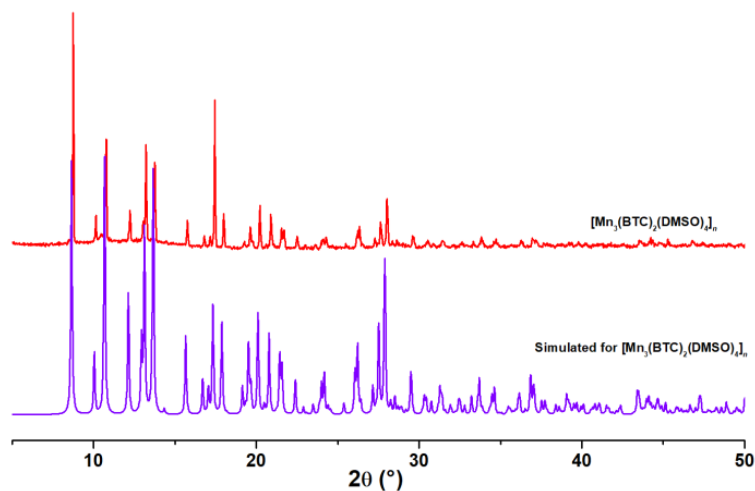


Figure 5. Diffractogram obtained from PXRD analysis of $[\text{Mn}_3(\text{BTC})_2(\text{DMSO})_4]_n$ (experimental) and diffractogram simulated from the data of SCXRD analysis of coordination network.

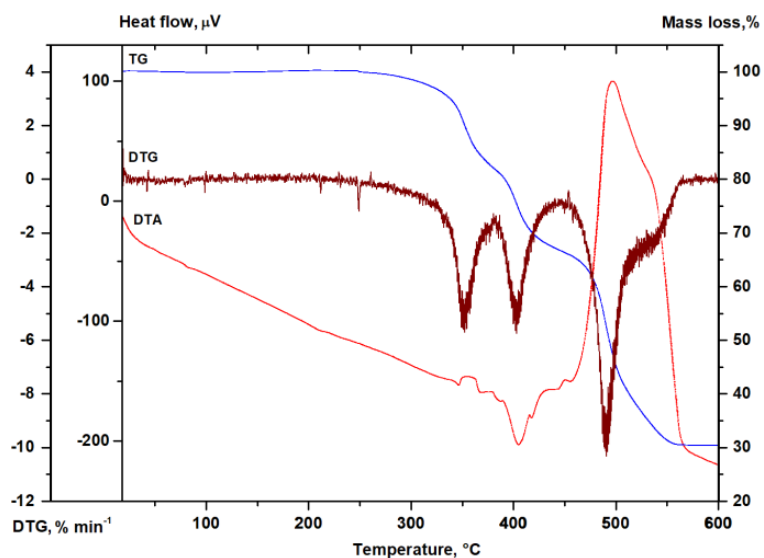


Figure 6. TG (blue), DTG (yellow) and DTA (red) curves obtained for the compound.

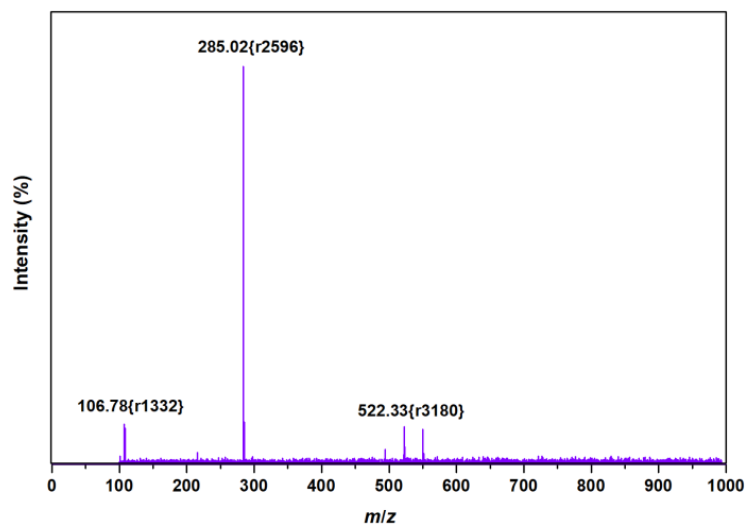


Figure 7. The spectrum obtained in the TOF-LDI analysis from a pure sample of $[\text{Mn}_3(\text{BTC})_2(\text{DMSO})_4]_n$.

4. Conclusion

Wanting to obtain a metal-organic framework with mixed ligands (acid-acid), through BTC and GLU, a novel tridimensional coordination network, based on Mn(II), BTC and DMSO ligand (μ_2 -O bridging) was obtained. Single crystal X-ray diffraction analysis provided significant insights as to the chemical crystalline structure, enabling topological studies. The reticular synthesis was verified in the context of the molecular building block approach and the junction of triangles and octahedra to assemble a tridimensional coordination network with rutile topology was observed. This RTL network can be classified as binodal, 3,6-connected, and exhibit a $(4.6^2)_2(4^2.6^{10}.8^3)$ point symbol with transitivity [22,32], obeying the *minimal transitivity principle*.

Spectroscopic analysis of the $\Delta\nu = [\nu(\text{COO})_{\text{as}} - \nu(\text{COO})_{\text{s}}]$ parameter suggests that the carboxylate group from BTC ligand was involved in two distinct coordination modes, bridge, and bidentate chelate. The thermal analysis suggested the stability of the material up to 250 °C and PXRD reinforced the purity of the crystalline phase, whereas the single crystal analysed for the crystal structure determination was representative of the entire. The TOF-MS/LDI experiment showed that $[\text{Mn}_3(\text{BTC})_2(\text{DMSO})_4]_n$ absorbs the laser energy in $\lambda = 337$ nm and possesses a relation of desorption/ ionization, independent of the matrix, with the most abundant peak at m/z 285. These results suggest the potential application of the compound as a matrix for the analysis of small molecules.

Acknowledgments

The authors wish to thank the Brazilian Research Development Agencies: CNPq, CAPES, and FAPEMIG (CEX-APQ-00947-14 and CEX-APQ-01283-14) for financial support.

Supporting information

CCDC-1902199 contains the supplementary crystallographic data for this paper. These data can be obtained free of charge via <https://www.ccdc.cam.ac.uk/structures/>, or by emailing data_request@ccdc.cam.ac.uk, or by contacting The Cambridge Crystallographic Data Centre, 12 Union Road, Cambridge CB2 1EZ, UK; fax: +44(0)1223-336033.

Disclosure statement

Conflict of interests: The authors declare that they have no conflict of interest.

Ethical approval: All ethical guidelines have adhered.

Sample Availability: Samples of the compounds are available from the author.

ORCID

Leoná da Silva Flores

 <http://orcid.org/0000-0002-1092-8182>

Roselia Ives Rosa

 <http://orcid.org/0000-0002-5801-7919>

Jefferson da Silva Martins

 <http://orcid.org/0000-0003-4499-8549>

Roberto Rosas Pinho

 <http://orcid.org/0000-0002-8637-6388>

Renata Diniz

 <http://orcid.org/0000-0001-9042-9094>

Charlane Cimini Corrêa

 <http://orcid.org/0000-0002-7113-8870>

References

- [1]. Schultz, J. L.; Wilks, E. S. Encyclopedia Of Polymer Science and Technology, 4th edition, John Wiley & Sons, 2005.
- [2]. Ohrstrom, L.; Kemiteknik, I. K.; Hogs kola, C. T.; Gothenburg, S. *Crystals* **2015**, *5*, 154-162.
- [3]. Batten, S. R.; Champness, N. R.; Chen, X.-M.; Garcia-Martinez, J.; Kitagawa, S.; Öhrström, L.; O'Keeffe, M.; Paik Suh, M.; Reedijk, J. *Pure Appl. Chem.* **2013**, *85*, 1715-1724.
- [4]. Tranchemontagne, D. J.; Ni, Z.; Keffe, M. O.; Yaghi, O. M. *Angewandte*. **2008**, *47*, 5136-5147.
- [5]. O'Keeffe, M. *Chem. Soc. Rev.* **2009**, *38*, 1215-1217.
- [6]. Ockwig, N. W.; Delgado-Friedrichs, O.; O'Keeffe, M.; Yaghi, O. M. *Acc. Chem. Res.* **2005**, *38*, 176-182.
- [7]. Zhang, W. X.; Liao, P. Q.; Lin, R. B.; Wei, Y. S.; Zeng, M. H.; Chen, X. M. *Coord. Chem. Rev.* **2015**, *293-294*, 263-278.
- [8]. DeCoste, J. B.; Peterson, G. W.; Jasuja, H.; Glover, T. G.; Huang, Y.; Walton, K. S. *J. Mater. Chem. A* **2013**, *1*, 5642-5650.
- [9]. O'Keeffe, M.; Eddaoudi, M.; Li, H.; Reineke, T.; Yaghi, O. M. *J. Solid State Chem.* **2000**, *152*, 3-20.
- [10]. Furukawa, H.; Kim, J.; Ockwig, N. W.; O'Keeffe, M.; Yaghi, O. M. *J. Am. Chem. Soc.* **2008**, *130*, 11650-11661.
- [11]. Yaghi, O. M.; O'Keeffe, M.; Ockwig, N. W.; Chae, H. K.; Eddaoudi, M.; Kim, J. *Nature* **2003**, *423*, 705-714.
- [12]. Li, M.; Li, D.; O'Keeffe, M.; Yaghi, O. M. *Chem. Rev.* **2014**, *114*, 1343-1370.
- [13]. Kumar, K.; Murugesan, S. *J. Saudi Chem. Soc.* **2018**, *22*, 16-26.
- [14]. Lingensfelder, M.; Fuhr, J.; Gayone, J.; Ascolani, H. Encyclopedia of Interfacial Chemistry, Elsevier, 2018.
- [15]. Xu, L.; Kwon, Y. U.; De Castro, B.; Cunha-Silva, L. *Cryst. Growth Des.* **2013**, *13*, 1260-1266.
- [16]. Salavati-Niasari, M.; Soofivand, F.; Sobhani-Nasab, A.; Shakouri-Arani, M.; Yeganeh Faal, A.; Bagheri, S. *Adv. Powder Technol.* **2016**, *27*, 2066-2075.
- [17]. Park, H. J.; Suh, M. P. *Chem. Eur. J.* **2008**, *14*, 8812-8821.
- [18]. Du, M.; Jiang, X. J.; Zhao, X. J. *Chem. Commun. (Camb)*. **2005**, *44*, 5521-5523.
- [19]. Yin, Z.; Zhou, Y. L.; Zeng, M. H.; Kurmoo, M. *Dalton Trans.* **2015**, *44*, 5258-5275.
- [20]. Sheldrick, G. *Acta Crystallogr. A* **2008**, *64*, 112-122.
- [21]. Sheldrick, G. *Acta Crystallogr. C* **2015**, *71*, 3-8.
- [22]. Sheldrick, G. *Methods Enzymol.* **1997**, *276*, 628-641.
- [23]. Wońska, M.; Grabowsky, S.; Dominiak, P. M.; Woźniak, K.; Jayatilaka, D. *Sci. Adv.* **2016**, *2*, e1600192-e1600192.
- [24]. Lindon, J. C. Encyclopedia of Spectroscopy and Spectrometry, University of Durham, UK, Elsevier, 1999.
- [25]. Farrugia, L. J. *J. Appl. Cryst.* **2012**, *45*, 849-854.
- [26]. Farrugia, L. J. *J. Appl. Crystallogr.* **1997**, *30*, 565-565.
- [27]. Macrae, C. F.; Edgington, P. R.; McCabe, P.; Pidcock, E.; Shields, G. P.; Taylor, R.; Towler, M.; Van De Streek, J. *J. Appl. Cryst.* **2006**, *39*, 453-457.
- [28]. Mugheirbi, N. A.; Tajber, L. *Mol. Pharm.* **2015**, *12*, 3468-3478.
- [29]. Blatov, V. A.; Shevchenko, A. P.; Serezhkin, V. N. *J. Appl. Crystallogr.* **2000**, *33*, 1193-1193.
- [30]. Blatov, V. A.; Shevchenko, A. P.; Proserpio, D. M. *Cryst. Growth Des.* **2014**, *14*, 3576-3586.
- [31]. Fedorov, A. V.; Shamanaev, I. V. *Mol. Inform.* **2017**, *36*, 1-8.
- [32]. Zhang, S.; Hua, Y.; Chen, Z.; Zhang, S.; Hai, H. *Inorganica Chim. Acta* **2018**, *471*, 530-536.
- [33]. Rardin, R. L.; Poganiuch, P.; Bino, A.; Goldberg, D. P.; Tolman, W. B.; Liu, S.; Lippard, S. J. *J. Am. Chem. Soc.* **1992**, *114*, 5240-5249.
- [34]. Yang, Y. Q.; Zhang, M. B.; Chen, M. S.; Chen, Z. M. *Zeitsch. Naturforsch. B* **2012**, *67*, 209-212.
- [35]. Jeong, S.; Song, X.; Jeong, S.; Oh, M.; Liu, X.; Kim, D.; Moon, D.; Lah, M. S. *Inorg. Chem.* **2011**, *50*, 12133-12140.
- [36]. Fomina, I.; Dobrokhotova, Z.; Aleksandrov, G.; Emelina, A.; Bykov, M.; Malkerova, I.; Bogomyakov, A.; Puntus, L.; Novotortsev, V.; Eremenko, I. *J. Solid State Chem.* **2012**, *185*, 49-55.
- [37]. Hoffman, A. E. J.; Vanduyfhuys, L.; Nevjestic, I.; Wieme, J.; Rogge, S. M. J.; Depauw, H.; Van Der Voort, P.; Vrielinck, H.; Van Speybroeck, V. *J. Phys. Chem. C* **2018**, *122*, 2734-2746.
- [38]. Zhang, Y. B.; Furukawa, H.; Ko, N.; Nie, W.; Park, H. J.; Okajima, S.; Cordova, K. E.; Deng, H.; Kim, J.; Yaghi, O. M. *J. Am. Chem. Soc.* **2015**, *137*, 2641-2650.
- [39]. Bonneau, C.; Delgado-friedrichs, O.; Keffe, M. O.; Omar, M.; Bonneau, C.; Delgado-friedrichs, O.; Keffe, O. *Acta Crystallogr. A* **2004**, *60*, 517-520.
- [40]. Cotton, F. A.; Francis, R.; Horrocks, W. D. *J. Phys. Chem.* **1960**, *64*, 1534-1536.
- [41]. Chen, L.; Mowat, J. P. S.; Fairen-Jimenez, D.; Morrison, C. A.; Thompson, S. P.; Wright, P. A.; Düren, T. *J. Am. Chem. Soc.* **2013**, *135*, 15763-15773.
- [42]. Nakamoto, K. Infrared and Raman Spectra of Inorganic and

- Coordination Compounds: Part A, 6th edition, John Wiley & Sons, 2009.
- [43]. Nakamoto, K. Infrared and Raman Spectra of Inorganic and Coordination Compounds: Part B, 6th edition, John Wiley & Sons, 2009.
- [44]. Carbone, E.; Mesquita, C.; Bille, E.; Day, N.; Dauphin, B.; Beretti, J. L.; Ferroni, A.; Gutmann, L.; Nassif, X. *J. Clin. Biochem.* **2011**, *44*, 104-109.
- [45]. Guo, Z.; He, L. *Anal. Bioanal. Chem.* **2007**, *387*, 1939-1944.
- [46]. Guo, Z.; Zhang, Q.; Zou, H.; Guo, B.; Ni, J. *Anal. Chem.* **2002**, *74*, 1637-1641.
- [47]. Cohen, L. H.; Gusev, A. I. *Anal. Bioanal. Chem.* **2002**, *373*, 571-586.
- [48]. Wang, S.; Niu, H.; Zeng, T.; Zhang, X.; Cao, D.; Cai, Y. *Microporous Mesoporous Mater.* **2017**, *239*, 390-395.



Copyright © 2019 by Authors. This work is published and licensed by Atlanta Publishing House LLC, Atlanta, GA, USA. The full terms of this license are available at <http://www.eurjchem.com/index.php/eurjchem/pages/view/terms> and incorporate the Creative Commons Attribution-Non Commercial (CC BY NC) (International, v4.0) License (<http://creativecommons.org/licenses/by-nc/4.0>). By accessing the work, you hereby accept the Terms. This is an open access article distributed under the terms and conditions of the CC BY NC License, which permits unrestricted non-commercial use, distribution, and reproduction in any medium, provided the original work is properly cited without any further permission from Atlanta Publishing House LLC (European Journal of Chemistry). No use, distribution or reproduction is permitted which does not comply with these terms. Permissions for commercial use of this work beyond the scope of the License (<http://www.eurjchem.com/index.php/eurjchem/pages/view/terms>) are administered by Atlanta Publishing House LLC (European Journal of Chemistry).